Exploring the Interaction of a Micelle Entrapped Biologically Important Proton Transfer Probe with the Model Transport Protein Bovine Serum Albumin

ARTICLE *in* THE JOURNAL OF PHYSICAL CHEMISTRY B · JULY 2014

Impact Factor: 3.3 · DOI: 10.1021/jp504037y · Source: PubMed

4 AUTHORS, INCLUDING:

Ashis Kundu
University of Calcutta
16 PUBLICATIONS **41** CITATIONS
SEE PROFILE

Animesh Pramanik
University of Calcutta
100 PUBLICATIONS **751** CITATIONS
SEE PROFILE

THE JOURNAL OF PHYSICAL CHEMISTRY B

Article

pubs.acs.org/JPCB

Exploring the Interaction of a Micelle Entrapped Biologically Important Proton Transfer Probe with the Model Transport Protein Bovine Serum Albumin

Debarati Ray, Ashis Kundu, Animesh Pramanik, and Nikhil Guchhait*

Department of Chemistry, University of Calcutta, 92 A. P. C. Road, Kolkata, 700009, India

Supporting Information

ABSTRACT: This article describes the interaction of a micelle entrapped pharmaceutically important isoindole fused imidazole derivative, namely, 1-(2-hydroxy-5-methylphenyl)-3,5-dioxo-1*H*-imidazo-[3,4-*b*] isoindole (ADII), with the model transport protein bovine serum albumin (BSA). Different spectroscopic techniques such as steady state absorption, emission, circular dichroism, dynamic light scattering, etc., have been employed to explore preferential interaction of this drug template with micelles and protein BSA. Binding of ADII with BSA is found to be enormously modified when it is released from the micellar environment. The binding constant of the ADII−BSA complex is reduced when the probe is released from anionic SDS micelle, whereas the binding is observed to be strengthened in cationic CTAB micellar medium due to the formation of a 1:2 complex (ADII−BSA). Time-resolved studies also support our steady state findings that the released drug from the micellar environment is found to be strongly bound with the protein BSA. Circular dichroism (CD) and dynamic light scattering (DLS) study reveals that the secondary structure of BSA gets some stabilization in SDS medium after binding of drug template to protein. The probable binding location of the probe within the protein cavity (hydrophilic subdomain IA) has been explored from an AutoDock-based blind docking simulation study.

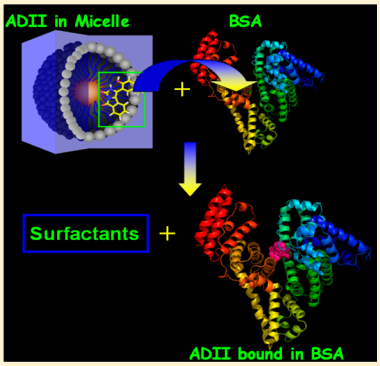

1. INTRODUCTION

Recent time has witnessed a tremendous evolution of research regarding the characterization of interaction of various potential drugs with different biological and biomimicking assemblies. This is because of the promising prospects of organized assemblies on the biological, photochemical, and photophysical processes.[1] Micelles are one of such organized assemblies that are widely used in medicinal chemistry for improving the solubility of sparingly soluble drugs in aqueous media, and they are formed above a critical concentration of surfactant, known as the critical micellar concentration (CMC).[2] Besides improving the solubility and bioavailability of drugs, the use of micelles as drug carriers is another advantage, as they are nontoxic, are permeable, and have a longer residence time in the system. Before using a biologically active compound as a drug, its interaction with different heterogeneous media (micelles, lipid, bilayer vesicles, biomembranes) should be carefully judged, as upon entrapment of the compound within the said medium it may induce some modification in its physicochemical properties, which may result in some undesirable side effects. In the literature, there are many studies in this particular area which are not only focused on designing various drug delivery systems, but they are also emphasizing the various routes for releasing the entrapped drugs from the delivery vehicles using external stimulations, such as ultrasonication, varying pH, temperature, etc.[3−5]

The present study deals with the investigation of the binding of a biologically important heterocyclic compound, a drug template, with the target protein bovine serum albumin (BSA) when the probe is released from the micellar environment. Serum albumins are the most widely studied proteins abundant in plasma and play a key role in the transport of various exogenous and endogenous compounds in the body. There are many reports on the knowledge of the nature and mechanism of interactions between the small molecules and proteins, as these have a crucial relevance to the understanding of biochemical consequences of drug−protein interactions.[6−11] Many researchers have studied the structure and properties of serum albumins and their interactions with other proteins in order to understand how serum albumins affect the functionality of foods containing proteins. The primary structure of bovine serum albumin (BSA) is composed of 583 amino acid residues and is characterized by low tryptophan content along with a high content of cystine, stabilizing a series of nine loops. The secondary structure of serum albumins has 67% of helix of six turns and 17 disulfide bridges.[11−14] The tertiary structure is composed of three domains I, II, and III, with each containing two subdomains A and B.[11−14] The protein BSA contains two tryptophan residues, Trp-134 and

Special Issue: Photoinduced Proton Transfer in Chemistry and Biology Symposium

Received: April 25, 2014
Revised: July 25, 2014

   dx.doi.org/10.1021/jp504037y | *J. Phys. Chem. B* XXXX, XXX, XXX−XXX

Trp-212, and they are located in the hydrophilic subdomain IB and hydrophobic subdomain IIA, respectively.[11−14]

In this article, we report the binding interaction of a pharmaceutically important isoindole fused imidazole derivative, namely, 1-(2-hydroxy-5methyl-phenyl)-3,5-dioxo-1*H*-imidazo-[3,4-*b*] isoindole (ADII), with the model transport protein BSA. Mainly, the interaction of different micelle-loaded drug template molecules with protein is focused on along with the probe−protein interaction in aqueous buffer medium in order to understand how the binding interaction is influenced in the presence of different types of surfactants, as the surfactants are also known to interact with the protein which causes modification of the structure of proteins, hence affecting the drug−protein interactions. The interactions of BSA with various surfactants have been previously studied and reported using various experimental techniques.[15−18]

The studied molecule ADII is known to exhibit an excited state intramolecular proton transfer process (ESIPT) through a four-member intramolecular hydrogen bonding network (vide Chart 1).[19] ADII yields dual emission in all organic solvents,

Chart 1. Schematic Representation of Lactim and Lactam Tautomerization of ADII Compound and the Possible Anionic Lactam Form

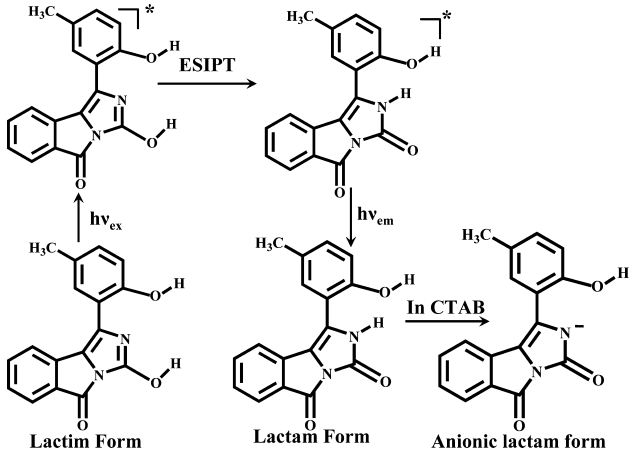

one corresponding to lactim emission (local emission, LE) and another for the lactam emission (proton transfer emission, PT). Both steady state and time-resolved fluorescence measurements suggest that the ESIPT process in ADII is less favorable in water than in other organic solvents.[19] The title compound ADII is widely used as a template to design various biologically active agents in medicinal chemistry.[20] Generally, imidazole-based heterocyclic molecules play an important role in various biochemical processes too.[21−24] In our previous study,[25] we have seen the differential binding interactions of ADII with the three micellar environments, e.g., sodium dodecyl sulfates (SDS), cetyltrimethylammonium bromide (CTAB), and Triton X-100 (TX-100), and the calculated high binding constant in these mediums justifies the application of three different types of micelles as its carrier. Here three different micelle (SDS, CTAB, and TX-100)-loaded ADII are subjected to interact with the plasma protein BSA to investigate the behavior of the released drug from the three different environments in the proteneous medium. For this purpose, we have mainly used steady state absorption, emission spectroscopy, circular dichroism, and dynamic light scattering study. The Auto-Dock-based "blind docking" simulation has been exploited to delineate the probable binding location of the drugs within the protein micro-heterogeneous cavity.

2. EXPERIMENTAL SECTION

2.1. Materials. The title compound 1-(2-hydroxy-5-methyl-phenyl)-3,5-dioxo-1*H*-imidazo-[3,4-*b*] isoindole (ADII) was synthesized as was reported by A. Pramanik and co-workers.[20] BSA (fatty acid free) from Sigma Chemical Co., USA, was used as received. The surfactants sodium dodecyl sulfates (SDS), cetyltrimethylammonium bromide (CTAB), and Triton X-100 (TX-100) have been purchased from Sigma Chemical Co. and were used without further purification. Tris buffer was purchased from SRL, India, and 0.01 M Tris−HCl buffer of pH 7.4 was prepared in triply distilled deionized water from a Milli-Q water purification system (Millipore). The solvent appeared visually transparent, and the purity of the solvent was also tested by running the fluorescence spectra in the studied wavelength range. Hydrochloric acid (HCl) from E-Merck was used as obtained.

2.2. Instrumentation and Methods. *2.2.1. Steady State Spectral Measurement.* The absorption and emission spectra have been recorded on a Hitachi UV−vis U-3501 spectrophotometer and a PerkinElmer LS55 fluorimeter, respectively. All spectra were recorded with appropriate background corrections. The concentrations of the protein (BSA) used in different experiments have been specified in the context. The concentration of ADII was fixed at ∼4.0 μM, and the pH is fixed at 7.40 throughout the study. All the experiments were carried out at room temperature (300 K).

The inner filter effect correction has been made for all the fluorescence spectra presented in the manuscript according to the following equation:[26]

$$I = I_{obs} \times \text{antilog}\left[\frac{1}{2}(A_{ex} + A_{em})\right] \quad (1)$$

Here, I and I_{obs} are the corrected fluorescence intensity and the observed background-subtracted fluorescence intensity of the sample under investigation, respectively. A_{ex} and A_{em} are the measured absorbance of the sample at the excitation and emission wavelengths, respectively.

2.2.2. Time-Resolved Measurements. The time-resolved fluorescence decay data have been measured on a FluoroCube-01-NL spectrometer based on the time-correlated single photon counting (TCSPC) technique using a laser diode at 450 nm as the light source to excite the lactam form of ADII, and the signals have been collected at a magic angle of 54.7°. The decays have been deconvoluted and analyzed by DAS-6 decay analysis software. The mean (average) fluorescence lifetime ($\langle\tau_{i0}\rangle$) has been calculated from the equation[26]

$$\langle\tau_{i0}\rangle = \frac{\sum_i \alpha_i \tau_i^2}{\sum_i \alpha_i \tau_i} \quad (2)$$

in which α_i represents the relative amplitude of the ith component of decay having the characteristic decay time constant τ_i, such that $\sum_i \alpha_i = 1$. The quality of the fits has been judged from χ^2 criterion and visual inspection of the residuals of the fitted functions to the actual data.

For time-resolved anisotropy measurements, the fluorescence decay curves were recorded at vertical and horizontal positions of the polarizer and analyzed by the following equations:[26]

dx.doi.org/10.1021/jp504037y | J. Phys. Chem. B XXXX, XXX, XXX−XXX

$$I_{\parallel}(t) = I(t)\frac{[1 + 2r(t)]}{3} \quad (3a)$$

$$I_{\perp}(t) = I(t)\frac{[1 - r(t)]}{3} \quad (3b)$$

where $I_{\parallel}$ and $I_{\perp}$ are the intensities collected at emission polarizations parallel and perpendicular, respectively, to the polarization axis of the excitation beam. $I(t)$ and $r(t)$ are the time-dependent intensity (at the magic angle) and anisotropy decay, respectively. Thus, the anisotropy decay function $r(t)$ has been constructed from these $I_{\parallel}(t)$ and $I_{\perp}(t)$ decays:[26]

$$r(t) = \frac{[I_{\parallel}(t) - GI_{\perp}(t)]}{[I_{\parallel}(t) + 2GI_{\perp}(t)]} \quad (4a)$$

where G is the correction factor which is defined as

$$G = \frac{I_{\perp}}{I_{\parallel}} \quad (4b)$$

2.2.3. Dynamic Light Scattering. Dynamic light scattering (DLS) measurements have been carried out on a Malvern Nano-ZS instrument employing a 4 mW He−Ne laser (λ = 632.8 nm) and attached with a thermostat sample chamber. The sample solution was poured into a DTS0112 low volume disposal cuvette of 1.5 mL (path length 1 cm). The operating procedure was programmed by the DTS software in a fashion that there was an average of 25 runs, with each run being averaged for 15 s and then a particular hydrodynamic diameter and size distribution extracted using the DTS software.

All experiments have been performed at ambient temperature of 300.0 K.

2.2.4. Circular Dichroism Measurements. The CD spectra of aqueous buffer solutions of BSA in the presence of surfactants and ADII were recorded by using a quartz cuvette of 1 mm path length with a Jasco J-815 CD spectrophotometer at 300.0 K room temperature. The mean residual ellipticities (MREs) or molar ellipticities at 208 nm were calculated using the following relation:

$$\text{MRE (deg·cm}^2\text{·dmol}^{-1}) = \frac{\theta_{obs}}{C_p nl \times 10} \quad (5)$$

in which θ_{obs} is the observed ellipticity in mdeg, C_p is the molar concentration of the protein, n is the number of amino acid residues (583 for BSA), and l is the cell path length (here 0.1 cm). The helicity content of the protein is then determined from the calculated MRE values at 222 nm using the following equation:[27]

$$\%\ \alpha\text{-helix} = \frac{-(\text{MRE} - 2340)}{30300} \times 100 \quad (6)$$

2.3. Molecular Modeling: Blind Docking Simulation. The native structure of BSA was taken from the Protein Data Bank having PDB ID 3V03. Docking studies were performed with the AutoDock 4.2 suite of programs which utilizes the Lamarckian genetic algorithm (LGA) implemented therein. For docking of ADII with BSA, the required file (corresponding to the three-dimensional structure of the drugs) for the ligand (ADII) was created through the combined use of the Gaussian 03W and AutoDock 4.2 software packages. The geometry of ADII was first optimized at the DFT//B3LYP/6-311+G(d,p) level of theory using the Gaussian 03W suite of programs, and the resultant geometry was then read in AutoDock 4.2 software in compatible file format, from which the required file was generated in AutoDock 4.2. The grid size was set to 126, 126, and 126 along the *X*-, *Y*-, and *Z*-axis with a 0.414 Å grid spacing; i.e., in order to recognize the binding sites of ADII in BSA, blind docking was performed. The AutoDocking parameters used were as follows: GA population size = 150; maximum number of energy evaluations = 250 000; GA crossover mode = two points. The lowest binding energy conformer was searched out of 10 different conformations for each docking simulation, and the resultant minimum energy conformation was applied for further analysis. The PyMOL software package was used for visualization of the docked conformations.[28]

3. RESULTS AND DISCUSSION

Before going to the detailed discussion on the interaction of BSA with free drug and with micelle-loaded drug, the understanding of the interaction of studied surfactants (which are drug carriers) with the protein is an important and essential task in order to understand the change of intrinsic spectral properties and conformation of BSA in the presence of the drug-carrier micelles (here surfactants, SDS, CTAB, and TX-100). The concentrations of the surfactants used for this purpose are the concentrations at the saturation level of interaction of ADII with the corresponding surfactant, and at these concentrations, all surfactants remain as the micellar form in pure aqueous buffer (Tris) medium.

3.1. Intrinsic Spectral Property, Structural and Conformational Change of BSA in the Presence of Surfactants. *3.1.1. Circular Dichroism (CD).* Far-UV CD spectroscopy gives the quantitative information regarding the change in secondary structure of BSA upon interaction with the studied surfactants. Figure 1 shows the far-UV CD spectra of pure BSA in aqueous buffer medium and in the presence of SDS, CTAB, and TX-100 surfactants. The CD spectrum of native BSA consists of two peaks in the ranges 208−209 and 221−223 nm, characteristic of the α-helix structure of BSA.[27,29−32] As seen in the figure, in the presence of surfactants, the decrease of the CD signal of the far-UV CD spectral profile of BSA is observed with no significant shifting of the peak positions. These results primarily indicate some sort of conformational change in the BSA secondary structure due to the interaction with surfactant molecules. The lowering in the negative ellipticity points toward a decrease in the α-helical content, which dictates the change of protein secondary structure of the protein. The estimated α-helicity content of

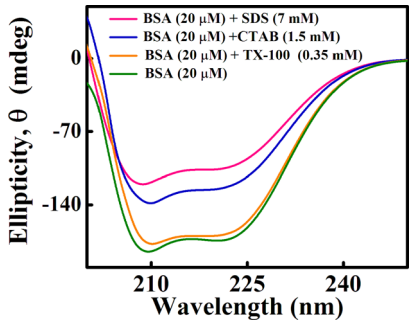

Figure 1. Far-UV circular dichroism spectral profiles of the protein BSA (20.0 μM) in the presence of SDS, CTAB, and TX-100.

dx.doi.org/10.1021/jp504037y | J. Phys. Chem. B XXXX, XXX, XXX−XXX

native BSA in Tris−HCl buffer (pH 7.40 and at T = 298 K) comes out to be ∼67%, which is in reasonable agreement with the literature reports.[29−32] In the presence of different surfactants, the α-helical content decreases from 67 to 45, 52, and 64 in 7 mM SDS, 1.5 mM CTAB, and 0.35 mM TX-100 medium, respectively. Therefore, CD spectroscopy suggests that in the presence of studied concentrations of surfactant a change of secondary structure of native protein results and the order of change is the maximum in SDS medium.

3.1.2. Emission Spectroscopy. The intrinsic fluorescence of BSA mainly arises due to the presence of two tryptophan residues, viz., Trp-212 and Trp-134. The protein (BSA) contains other fluorescent residues, e.g., phenylalanine (Phe) and tyrosine (Tyr), but the intrinsic fluorescence property of the native protein is mainly governed by the strong fluorescence of Trp residues. Figure 2 displays the intrinsic

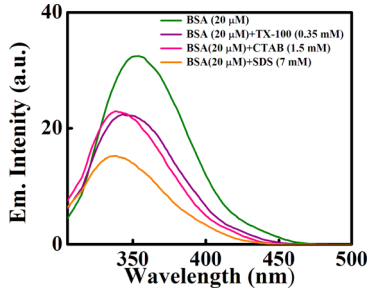

Figure 2. Modulation of intrinsic tryptophanyl fluorescence of BSA ([BSA] = 20.0 μM, λ_{ex} = 295 nm, pH 7.4 in Tris−HCl buffer) in the presence of SDS, CTAB, and TX-100 at a representative temperature T = 300 K.

tryptophenyl fluorescence spectra of BSA in aqueous buffer medium and in three surfactant (SDS, CTAB, and TX-100) media. It is found that, upon interaction of surfactants, a regular quenching process of the tryptophenyl fluorescence intensity of BSA is observed with a blue-shifting of emission maxima. The interactions of SDS, CTAB, and TX-100 with albumin protein have been previously monitored using fluorescence quenching of intrinsic tryptophans and circular dichroism spectroscopy, and a blue-shift in tryptophenyl fluorescence emission maxima is observed. The extent of fluorescence quenching and the shifting of emission maxima of BSA in the presence of studied surfactants are different. More specifically, in 7 mM SDS, the fluorescence intensity of BSA is quenched up to 63% of the initial value, whereas, in CTAB (1.5 mM) and TX-100 (0.35 mM) medium, it decreases to 37 and 25% of the initial value, respectively. Along with the significant quenching process, the tryptophenyl fluorescence maxima are also largely blue-shifted in SDS medium compared to the other surfactant media (λ_{em}^{max} shifts from 350 nm (in aqueous medium) to 335 (in SDS), 338 (CTAB), and 344 nm (in TX-100)). The blue-shift of emission maxima of BSA in the presence of surfactants signifies the fact that the hydrophobicity in the vicinity of the tryptophan residue increases upon a change of secondary structure induced by the surfactant molecule.[33,34]

3.1.3. Dynamic Light Scattering (DLS). Dynamic light scattering (DLS) measurement provides an effective way to investigate the interaction of BSA with the surfactant from the modification of the dimensions of macromolecular protein structure. Figure 3 displays the intensity distribution of DLS profiles of BSA in aqueous buffer medium and in the presence of different surfactant media (7 mM SDS, 1.5 mM CTAB, and

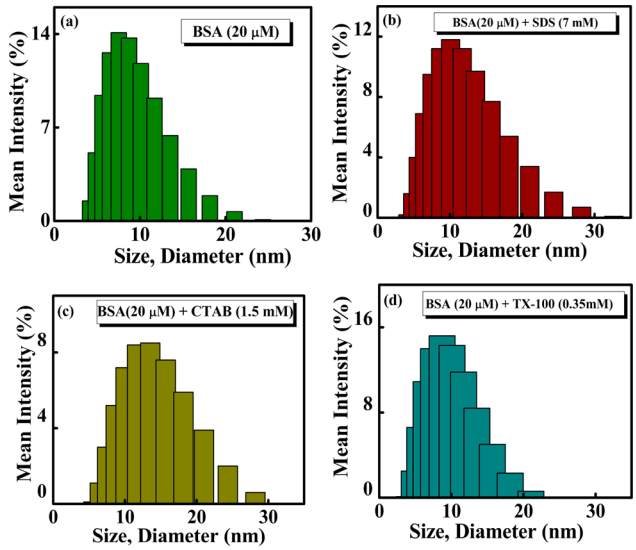

Figure 3. Size distribution graph for BSA in aqueous buffer solution and in the presence of SDS, CTAB, and TX-100 medium at pH 7.4.

0.35 mM TX-100). The DLS profile of native BSA at 300 K shows two peaks with hydrodynamic diameters of 7.4 and 135 nm. The first peak at 7.4 nm corresponds to the hydrodynamic diameter of native BSA (monomer), whereas the peaks at higher hydrodynamic diameter may be due to the presence of BSA oligomers/aggregates (Figure S1, Supporting Information). Under our experimental conditions, all the surfactant molecules remain as a micellar form in the pure aqueous buffer medium, and from the literature report,[35] we found that the hydrodynamic radii of SDS, CTAB, and TX-100 micelles are 2.07, 2.57, and 4.40 nm, respectively. The obtained hydrodynamic radii (R_h's) of native BSA, BSA−SDS system, BSA−CTAB system, and BSA−TX-100 system are found to be 3.7, 5.0, 6.7, and 4.1 nm, respectively (Table 1). Therefore, from

Table 1. Summary of the Obtained Hydrodynamic Radii (R_h) and the Percentage Change of α-Helix Content of the Protein during the ADII−BSA Binding Interaction Process in Aqueous Tris Buffer Medium and Different Surfactant Media

environment	[BSA] (μM)	[ADII] (μM)	hydrodynamic radius (R_h)[a] (nm)	α-helix[b] (%)
aqueous buffer	20		3.7	67
		4	4.1	65
SDS	20		5.0	45
		4	4.3	55
CTAB	20		6.7	52
		4	6.8	53
TX-100	20		4.1	64
		4	4.3	63

[a]The error limit in the calculation of R_h is ±0.3 nm. [b]The error limit in the calculation of % α-helix is ±2.

these data (R_h of the BSA−surfactant system and the pure micelle of the surfactants), we cannot infer that the structures of the surfactants are disrupted in the presence of BSA, as these data are not far extreme from each other. However, it is reported in the literature[15−17] that, in the presence of BSA, the SDS and TX-100 surfactant molecules preferably form a BSA−

dx.doi.org/10.1021/jp504037y | J. Phys. Chem. B XXXX, XXX, XXX−XXX

surfactant complex and the surfactant molecules may aggregate on the protein surface. Therefore, the obtained hydrodynamic radii are due to the BSA−surfactant (BSA−SDS and BSA−TX-100) complexes. As the surfactant molecules aggregate on the protein surface, it induces a conformational change on the protein secondary structure. Therefore, our findings from the previous CD and fluorescence quenching experiment are justified. In the case of CTAB surfactant, the situation is quite different. The obtained hydrodynamic radius of the BSA−CTAB system is found to be almost twice that of the radius of the monomer of the native protein. In a recent article, Sharma et al.[18] have shown that, in the presence of CTAB, protein BSA aggregates. In the presence of CTAB, the protein gets unfolded and the unfolded form can polymerize in the solution to form soluble aggregates. This fact is confirmed by our experimental data presented in Figure S1 (Supporting Information), which shows that the BSA aggregation increases in the presence of CTAB surfactant. Therefore, we can say that, in the presence of CTAB, the aggregated dimeric form of BSA predominates and our obtained hydrodynamic radius of the BSA−CTAB system is in close harmony with the radius of the dimeric form of BSA.[36]

From the above results (emission, CD, and DLS study), we can infer that, in the presence of SDS, CTAB, and TX-100 surfactants, the native structure of BSA is partially changed and the extent of change is varied in different surfactant media. As BSA protein is not severely perturbed in any of the studied surfactant media, the study of the interaction of different micelle (SDS, CTAB, and TX-100)-loaded ADII with the BSA is justified; otherwise, it is meaningless if complete denaturation of BSA happened in the presence of the surfactants.

3.2. Binding Interaction of ADII with the Protein BSA in Aqueous Tris Buffer Medium. *3.2.1. Absorption and Emission Studies.* The absorption spectrum of ADII in Tris buffer (pH 7.4) medium shows a similar profile as was observed in water; i.e., the spectrum consists of mainly two bands at ∼305 nm and ∼400 nm which are assigned to the lactim and lactam form of ADII, respectively.[19,25] Figure 4a shows the absorption spectra of ADII in the presence of a varying concentration of BSA in aqueous buffer medium. Since ADII exists in both tautomeric forms (lactim and lactam) at our working pH condition, both forms can interact with the studied protein BSA. As the protein BSA shows a broad absorption band within the 250−310 nm wavelength range in Tris buffer medium, in this situation, it is very difficult to extract information regarding the changes of the lactim absorption band of ADII in the presence of BSA. On performing the same experiment using BSA solution as a blank, it is found that only a slight increase of the lactim absorption band is observed (the figure not shown). The lactam band of ADII is also found out to be insignificantly changed in the presence of BSA except for the slight broadening and increased absorbance which are presented in the inset of Figure 4a.

As the changes of the absorption spectral profile of ADII in the presence of BSA are not so prominent, we have performed a fluorescence study to follow the interaction between the two partners. The photophysical properties of ADII in the bulk homogeneous solvents have been previously reported by our laboratory.[19] The molecule ADII shows dual emissions at ∼420 nm and ∼490 nm at λ_{ex} = 320 nm (i.e., lactim excitation) in all organic solvents where the high energy emission was assigned to the lactim emission and the low energy emission due to the lactam form.[19,25] A single emission at ∼490 nm is found out

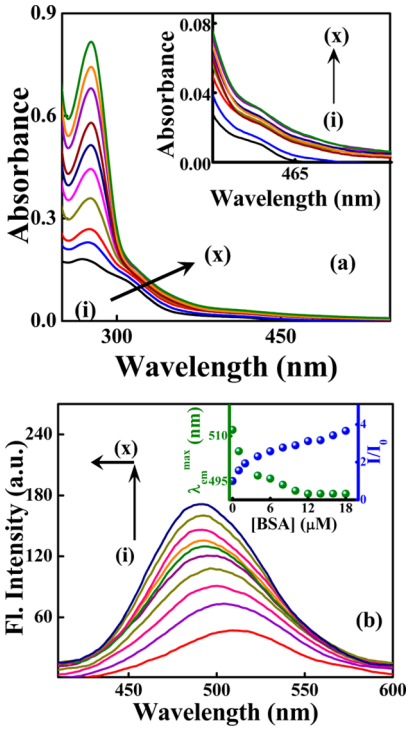

Figure 4. Representative (a) absorption and (b) emission spectral profile of the ADII in the presence of increasing protein (BSA) concentration. Curves i−x correspond to [BSA] (μM) = 0.0, 1.0, 2.0, 4.0, 6.0, 8.0, 10.0, 12.0, 16.0, and 20.0. Inset of Figure 4a shows the expanded view of the absorption spectra from 370 nm to 550 nm. Inset of Figure 4b shows the variation of emission maxima and relative intensity of ADII with BSA.

when only the lactam form is excited at 400 nm. As the absorption spectral band for the lactim form coincides with the absorption band of the Trp residue of BSA, we have followed only the modification of lactam emission of ADII in the presence of BSA to characterize the ADII−BSA interaction. In Tris aqueous buffer medium, the molecule ADII exhibits a broad emission band at 513 nm upon excitation at 400 nm (lactam band). Figure 4b displays a prominent enhancement of the lactam emission as a function of increasing protein BSA concentration with large blue-shifting of the emission maxima (from λ_{em} = 513 nm in bulk Tris buffer medium to 490 nm in 20 μM BSA). Such modulations of lactam emission of ADII in BSA medium definitely suggest that the microenvironment around the fluorophore becomes different in comparison to the bulk homogeneous aqueous (buffer) medium. The increase in the fluorescence intensity with a concomitant blue-shift reveals that the polarity in the immediate environment around the probe is definitely lowered pointing toward the encapsulation of the lactam form of ADII within the protein cavity.

3.3. Binding Interaction of Protein BSA with the Micelle-Loaded ADII. *3.3.1. Absorption and Emission Studies.* The interactions of ADII with all the surfactants under investigation (anionic, SDS; cationic, CTAB; neutral, TX-100) have been studied, and the details are reported in our previous publication.[25] The inherent prototropic transformation of ADII, i.e., the lactim−lactam tautomerism process, is found to be differentially modulated within the micellar assemblies, as reflected on the absorption and emission spectral profiles. From the previous study, it is clear that the prototropic transformation of ADII in the anionic micellar medium SDS is

dx.doi.org/10.1021/jp504037y | J. Phys. Chem. B XXXX, XXX, XXX−XXX

more favored toward the lactam form of ADII, as evidenced from the increase of absorbance of the lactam band (λ_{abs} = 400 nm). However, the modification on the absorption profile of the probe in the presence of the cationic (CTAB) micellar medium suggests that the neutral ADII molecule becomes anionic due to the deprotonation of hydrogen attached to the nitrogen atom of the lactam form which is reflected from the generation of a new band at ~475 nm in the presence of CTAB. Such modulations of the absorption spectra of ADII indicate that the ground state intramolecular prototropic equilibrium (lactim−lactam conversion) of ADII is modified in the micro-heterogeneous environments of the surfactants compared to that in the aqueous buffer phase.

The modifications of the absorption spectra of three different micelle (SDS, CTAB, and TX-100)-bound ADII in the presence of an increasing concentration of BSA are shown in Figure 5. In SDS and TX-100 medium, no such interesting

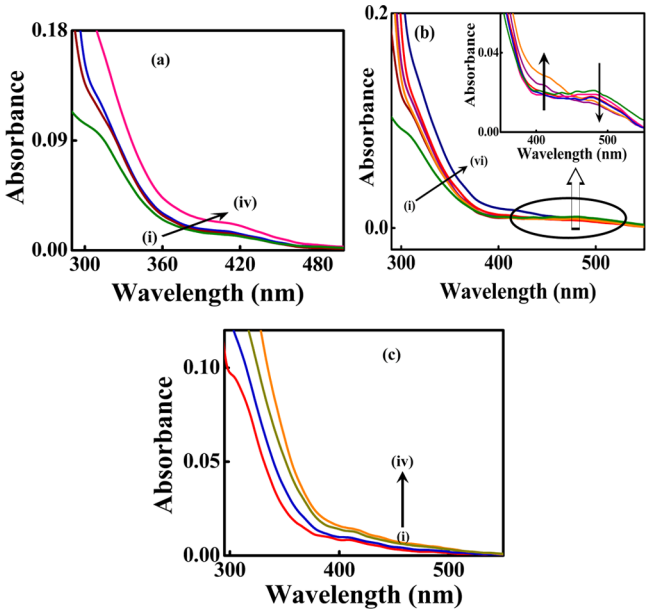

Figure 5. Representative absorption spectral profile of the micelle-bound [(a) SDS (7 mM), (b) CTAB (1.5 mM), the inset shows the magnified view of the marked region, and (c) TX-100 (0.35 mM)] ADII in the presence of increasing protein (BSA) concentration. Curves i−iv and i−vi correspond to [BSA] (μM) = 0.0, 4.0, 8.0, and 16.0 and 0.0, 2.0, 6.0, 8.0, 10.0, 16.0, and 20.0, respectively.

spectral modulation is observed except for a slight increment of the lactam absorption band at ~400 nm (Figure 5a and c). However, interesting results are observed when cationic-micelle-bound ADII is placed in BSA medium. It is found that addition of BSA to the cationic micellar medium of ADII results in a distinct reappearance of the absorbance of the neutral lactam band (λ_{abs} = 400 nm) with a decrement of the anionic lactam band intensity at ~475 nm (Figure 5b). This result suggests that the anionic ADII molecule definitely gains a proton from the protein medium to form the neutral lactam form.

The emission spectral profile of ADII was also found out to be vividly modified in the micellar medium.[25] In the presence of the anionic (SDS) and neutral (TX-100) surfactants, the excited state prototropic equilibrium of ADII was found to be favored more toward the lactam form, as manifested through the greater enhancement of the lactam fluorescence band at λ_{em} = 513 nm than the lactim band. The emission maxima of ADII are blue-shifted from 513 nm in aqueous buffer medium to 508 nm in SDS micellar medium and 500 nm in TX-100 medium at the saturation level of interaction of ADII with the respective micellar medium. In the cationic surfactant medium, the lactam emission intensity is gradually decreased up to the CMC of CTAB due to the deprotonation of the lactam form, but after the CMC, the encapsulated anionic lactam form is stabilized within the cationic micelle, as evidenced from the enhanced emission intensity of the anionic form with blue-shifting of emission maxima.

The emission spectra of the micelle-encapsulated ADII are found to be modified in the presence of an increasing concentration of BSA. When BSA is added to the ADII loaded SDS or TX-100 micellar medium, a blue-shift of emission maxima with a nominal increase of fluorescence intensity is observed (Figure 6a and c). In the presence of BSA, the

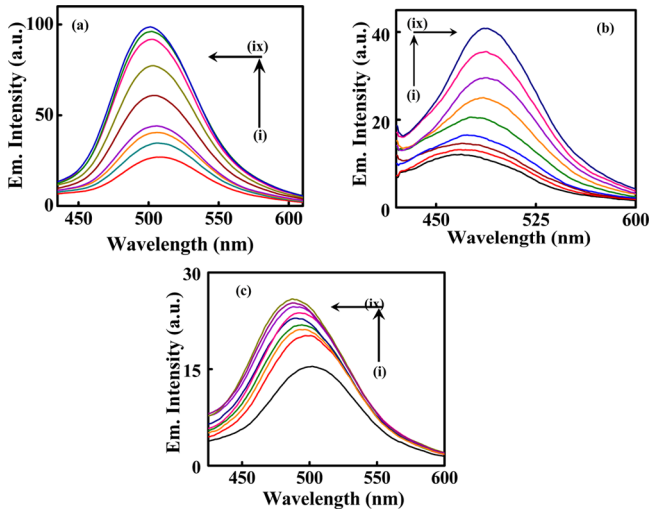

Figure 6. Representative emission spectral profile of the micelle-bound [(a) SDS (7 mM), (b) CTAB (1.5 mM), and (c) TX-100 (0.35 mM)] ADII in the presence of increasing protein (BSA) concentration. Curves i−ix correspond to [BSA] (μM) = 0.0, 2.0, 4.0, 6.0, 8.0, 12.0, 14.0, 16.0, and 20.0.

emission maxima of ADII shift from 508 nm (in 7 mM SDS) to 500 nm (in the presence of 20 μM BSA in 7 mM SDS medium) and from 501 nm (in 0.35 mM TX-100) to 488 nm (in the presence of 20 μM BSA in 0.35 mM TX-100). However, addition of BSA in cationic-micelle-bound ADII solution is found to yield a red-shift of emission maxima from 480 nm (in 1.5 mM CTAB) to 490 nm (in the presence of BSA in 1.5 mM CTAB) with enhancement of emission intensity (Figure 6b). Therefore, these results suggests that in the presence of BSA the encapsulated ADII molecules get released from the unit of the surfactants and bind with the BSA protein, as the molecule ADII has a commendable binding affinity with the protein. Therefore, the hypsochromic shift of the emission maxima of micelle (SDS/TX-100)-encapsulated ADII in the presence of BSA is thus justified as the polarity in the immediate binding site of ADII in the protein environment is further lowered than the micellar medium. As the emission maximum of the ADII−BSA complex lies at 500 nm in the SDS medium which is ~10 nm red shifted as compared to that in aqueous buffer phase (in aqueous buffer medium, λ_{em} of the ADII−BSA complex lies at ~490 nm), this suggests that in SDS medium the bound ADII

dx.doi.org/10.1021/jp504037y | J. Phys. Chem. B XXXX, XXX, XXX−XXX

in the protein cavity is more exposed to the bulk environment due to the partial unfolding of the protein secondary structure in the presence of the surfactant SDS. On the other hand, the red-shift of emission maxima of CTAB-micelle-loaded ADII in the presence of BSA seemed to be anomalous, as we have seen earlier that a hypsochromic shift is observed when the probe is bound to BSA. This behavior of ADII is explained by considering the fact that the molecule is anionic in CTAB micelle medium, but in the presence of BSA, it becomes neutral, as strongly supported by the absorption study. Therefore, with increasing concentration of BSA in the medium, the so formed neutral molecules are now subjected to bind with BSA and show λ_{em}^{max} at the same position, as was found in pure BSA in aqueous buffer medium.

3.4. Fluorescence Quenching Study. In this section, iodide ion (I^-) induced fluorescence quenching of BSA-bound ADII (both in aqueous and surfactant medium) has been exploited to get an idea about the accessibility of the entrapped probe molecule to the ionic quencher in the protein medium.[37] It is known that, being an ionic quencher, the iodide ion is preferentially available in the polar region of any medium and not supposed to be available in the hydrophobic interior of the protein.

The quenching rate constants for the different systems have been calculated using the very popular Stern–Volmer equation:[26]

$$\frac{I_0}{I} = 1 + K_{SV}[Q] \tag{7}$$

where I_0 and I are the fluorescence intensities of the fluorophore (ADII) in the absence and presence of quencher (here I^-), [Q] is the molar concentration of the quencher (here I^-), and K_{SV} is the Stern–Volmer quenching constant. The higher the magnitude of K_{SV}, the better the quenching process, which suggests a greater degree of exposure of the probe to the quencher. The Stern–Volmer plots for I^--ion-induced quenching of ADII in aqueous buffer and in 20 μM BSA medium are displayed in Figure 7, and the corresponding K_{SV} values are presented in Table 1. The obtained lower K_{SV} value in BSA medium definitely points toward the fact that the probe molecule must reside on the hydrophobic region of BSA, hence less accessible to the quencher (I^-).

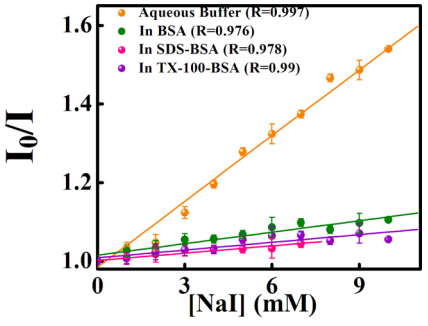

Figure 7. Stern–Volmer plot for iodide (I^-) ion induced fluorescence quenching of ADII in aqueous buffer, 7 mM SDS + 20 μM BSA, 1.5 mM CTAB + 20 μM BSA, and 0.35 mM TX-100 + 20 μM BSA.

A fluorescence quenching study has also been performed when various micelle-loaded ADII are placed in BSA medium. It is found that the obtained K_{SV} values in these cases are very close to the value obtained in aqueous BSA medium. Therefore, the ionic quencher induced fluorescence quenching study supports the fact that ADII molecule is definitely bound to the BSA after being released from the micellar assemblies.

3.5. Binding Interaction of BSA with the Lactam Form of ADII Dissolved in Aqueous and Various Medium. Binding constants for the binding of the free and micelle-loaded ADII with the plasma protein (BSA) have been determined to understand the degree of binding of the probe–protein (BSA) interaction process. The binding constant (K) for the ADII (lactam form)–BSA binding interaction and the free energy change (ΔG) for the process were determined using the well-known Benesi–Hildebrand equation.[38] The association constant of the complex has been determined from the following complexation equilibrium:

$$\text{ADII} + n\text{BSA} \leftrightarrow \text{ADII–BSA}n$$

Therefore, the equilibrium constant (K) can be written as

$$K = \frac{[\text{ADII–BSA}n]}{[\text{ADII}][\text{BSA}]^n} \tag{8}$$

Thus, Benesi–Hildebrand equations for 1:1 and 1:2 (where n = 2) complexes in terms of the fluorescence intensity of the probe can be written as

$$\frac{(I_\infty - I_0)}{(I - I_0)} = 1 + \frac{1}{K[\text{BSA}]} \tag{9}$$

$$\frac{(I_\infty - I_0)}{(I - I_0)} = 1 + \frac{1}{K[\text{BSA}]^2} \tag{10}$$

in which I_0, I, and I_∞ terms designate the emission intensities of the ADII, respectively, in the absence of BSA, at an intermediate concentration of BSA, and at the level of saturation of interaction. In the free aqueous buffer medium, the plot of $(I_\alpha - I_0)/(I - I_0)$ vs $1/[\text{BSA}]$ (M^{-1}) shows a linear regression, indicating the formation of a 1:1 stoichiometry between the probe (ADII) and the protein (BSA) (Figure 8). The binding constant (K) is determined from the slope of the

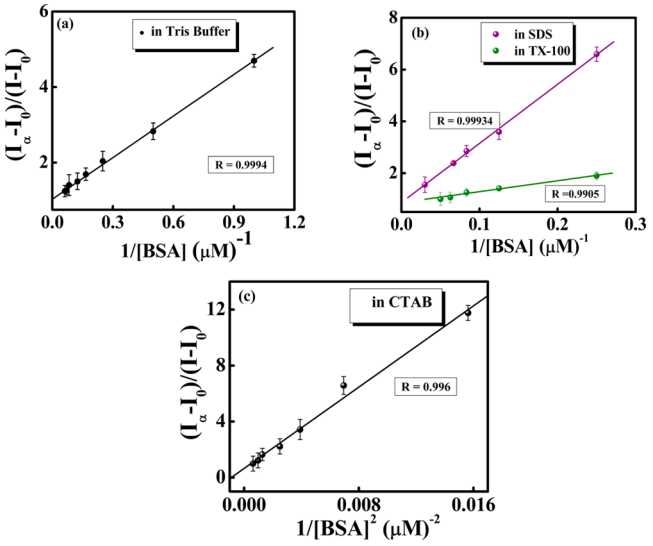

Figure 8. Benesi–Hildebrand plot of $(I_\alpha - I_0)/[I - I_0]$ vs $1/[\text{BSA}]$ for estimation of the binding constant of the probe (ADII)–protein (BSA) interaction in (a) aqueous buffer, (b) 7 mM SDS and 0.35 mM TX-100 medium assuming 1:1 complexation, and (c) 1.5 mM CTAB medium assuming 1:2 complexation.

dx.doi.org/10.1021/jp504037y | J. Phys. Chem. B XXXX, XXX, XXX–XXX

Table 2. Different Binding Parameters of the Lactam Form of ADII with the BSA in Aqueous Buffer Medium and Different Surfactant Medium at 27° C

host	guest	stoichimetry (host:guest)	binding constant	ΔG (kJ/mol)
BSA	ADII in aqueous buffer	1:1	2.7 (±0.4) × 10^5 M^{-1}	−31.2
BSA	SDS-loaded ADII	1:1	4.4 (±0.5) × 10^4 M^{-1}	−26.6
BSA	CTAB-loaded ADII	2:1	6.8 (±0.8) × 10^9 M^{-2}	−56.4
BSA	TX-100-loaded ADII	1:1	2.3 (±0.5) × 10^5 M^{-1}	−30.8

Table 3. Time-Resolved Fluorescence Lifetime Results of ADII in BSA, BSA−SDS, BSA−CTAB, and BSA−TX-100 Systems Collected at 525 nm

[BSA] (μM)	τ_1 (ns)	τ_2 (ns)	τ_3 (ns)	α_1	α_2	α_3	χ^2	$\langle\tau\rangle$ (ns)
Aqueous Buffer Medium								
0	1.61	7.41	0.148	0.03	0.02	0.95	1.16	3.55
4	1.63	7.68	0.137	0.09	0.07	0.84	1.20	5.48
6	1.68	7.67	0.144	0.10	0.08	0.82	1.09	5.56
8	1.64	7.62	0.137	0.12	0.08	0.80	1.17	5.45
10	1.71	7.79	0.142	0.13	0.08	0.79	1.15	5.48
12	1.76	7.85	0.154	0.13	0.08	0.79	1.11	5.47
SDS Medium								
0	0.863	5.88	0.181	0.67	0.03	0.30	1.09	1.91
4	0.914	5.40	0.264	0.61	0.06	0.33	1.09	2.35
6	1.04	5.59	0.310	0.54	0.08	0.38	1.09	2.77
8	1.22	5.76	0.332	0.51	0.11	0.38	1.10	3.22
10	1.45	5.95	0.314	0.48	0.15	0.37	1.12	3.73
CTAB Medium								
0	2.06	6.67	0.358	0.25	0.10	0.65	1.04	3.95
2	1.82	6.50	0.305	0.26	0.08	0.66	1.05	3.60
4	1.63	6.29	0.261	0.26	0.09	0.65	1.05	3.70
6	1.59	6.28	0.237	0.24	0.09	0.67	1.09	3.79
8	1.62	6.28	0.252	0.25	0.10	0.65	1.17	3.87
10	1.95	6.75	0.301	0.25	0.12	0.63	1.005	4.35
12	1.88	6.80	0.293	0.26	0.14	0.60	1.09	4.60
14	1.79	6.74	0.259	0.24	0.13	0.63	1.05	4.57
TX-100 Medium								
0	1.38	6.16	0.201	0.18	0.04	0.78	1.04	2.90
2	1.46	7.06	0.193	0.20	0.09	0.71	1.00	4.64
4	1.54	7.14	0.196	0.20	0.10	0.70	1.04	4.83
6	1.57	7.12	0.189	0.20	0.10	0.70	1.00	4.82
8	1.73	7.45	0.206	0.20	0.10	0.70	1.02	5.00
10	1.80	7.52	0.187	0.20	0.10	0.70	1.04	5.09

Benesi−Hildebrand plot, and the calculated high value of K (2.7 × 10^5 M^{-1}) indicates the strong binding affinity of the ADII toward BSA. The free energy change for this process of complexation also ($\Delta G = -RT \ln K = -31.2$ kJ·mol^{-1}, at experimental temperature (T) = 300 K) implies that the process of ADII−protein (BSA) binding interaction is thermodynamically favorable (negative free energy change).

The same eq 9 has been applied for the evaluation of binding constants of the ADII−BSA complex when the micelle-loaded ADII is placed in the protein medium. Figure 8 represents the B−H plot of the micelle (SDS/CTAB/TX-100)-bound ADII with BSA for the evaluation of the stoichiometry and the binding constants of the drug−protein complexes. From the analysis of fluorescence data of SDS- and TX-100-micelle-bound ADII with BSA, the B−H plots are found to reveal a 1:1 association of the complex (drug−protein). On the other hand, in cationic surfactant medium, the assumed 1:1 complexation between ADII (CTAB-micelle-bound) and BSA leads to a negative binding energy value, which strongly negates the possibility of a 1:1 ADII−BSA complex in CTAB medium. The obtained fluorescence data of cationic-micelle-bound ADII in BSA medium is found to be best fitted to 1:2 associations for the ADII−BSA complex (eq 10). The binding constant values (K) of the ADII−BSA complex are also distinctly modified in the presence of the studied surfactant medium (vide Table 1). The K value of TX-100-loaded ADII with BSA is found to be of the same order (2.3 × 10^5 M^{-1}) as obtained in aqueous buffer medium (2.7 × 10^5 M^{-1}), but in the presence of SDS surfactant, the obtained binding constant value is found to be 4.4 × 10^4 M^{-1}, which is almost 10 times lower than that obtained in pure aqueous BSA medium. On the other hand, a remarkably high binding constant (6.8 × 10^9 M^{-2}) for the 1:2 ADII−BSA complexation signifies a compact packing of the probe within the cavity space of the plasma protein BSA. Therefore, the modification of the binding constant for probe−BSA interaction thus can be utilized for the choice of a better drug carrier among the studied surfactants because the drug should be released from the transport protein to the target cell/tissue upon contact with them. This is only possible if the drug has a moderate binding affinity with the transported protein

dx.doi.org/10.1021/jp504037y | J. Phys. Chem. B XXXX, XXX, XXX−XXX

like BSA or HSA, so that the protein can easily carry the drug to the target site and release there.

3.6. Time-Resolved Studies. *3.6.1. Time-Resolved Fluorescence Lifetime Study.* In time-resolved studies, we will first discuss the change in lifetime of ADII in the presence of BSA in aqueous buffer medium. In aqueous buffer medium, the emission decay at 500 nm (at λ_{ex} = 450 nm) fits to a triexponential function with time constants of 0.148 ns (95%), 1.60 ns (2.6%), and 7.41 ns (2.4%). The first two components are due to the two conformers of the lactim form (closed and open form), whereas the slowest component is assigned to the excited lactam structure.[19] In the presence of BSA, the decay at 500 nm remains as a triexponential function (vide Figure S2, Supporting Information). Though the individual time constants of ADII remain almost unaltered, their relative amplitudes are vividly modified upon interaction with BSA (Table 3). The relative amplitudes of the excited state lactam form and the open lactim form are found to be increased from 2% (in aqueous buffer) to 8% and from 3% (in aqueous buffer) to 13% in 12 μM BSA, respectively. On the contrary, that of the shortest component (i.e., excited closed conformer of lactim form) decreases from 95% in aqueous buffer to 79% in 12 μM BSA. These results clearly indicate the presence of at least two emitters of ADII bound to BSA,[39] which is quite justified as both the lactim and lactam forms of ADII can be bound with the protein.

The time-resolved fluorescence decay profiles of different micelle (SDS, CTAB, and TX-100)-bound ADII in the presence of increasing concentrations of BSA at λ_{ex} = 450 nm and $\lambda_{monitored}$ = 515 nm are presented in Figure S3 (Supporting Information). When SDS-micelle-bound ADII is placed in BSA medium, the individual time constants of ADII and their relative amplitudes are noticeably varied with increasing protein concentration (vide Table 3). The relative amplitude of the excited state lactam form of ADII increases from 4 to 13% upon interaction with BSA with increasing lifetime, whereas the total population of the lactim form (closed + open form) decreases from 96 to 87%. In the case of the other two micelle (CTAB and TX-100)-bound ADII systems, similar kinds of results are found out, which are presented in Table 3.

3.6.2. Time-Resolved Fluorescence Anisotropy Decay. Time-resolved fluorescence anisotropy decay study often serves as an excellent indicator to assign the location of the probe in a multicomponent environment. To obtain further information regarding the microenvironment around the probe in the protein BSA medium, the time-resolved fluorescence anisotropy decay study of ADII in aqueous buffer as well as in protein environment has been performed and is presented in Figure 9. Here, also, we will first discuss the anisotropy decay of free aqueous ADII in BSA medium followed by the same in different micelle-bound ADII in BSA medium. ADII exhibits a single exponential decay profile in an aqueous buffer medium with a rotational relaxation time constant of 0.183 ns, as reported earlier,[25] but the anisotropy decay of ADII in the presence of varying concentrations of BSA is found to be quite interesting. At a lower concentration of protein BSA (2 and 6 μM), a growth component is observed which gives a "dip-and-rise" kind of anisotropy decay pattern. However, at higher protein concentration, this dip-and-rise kind of anisotropic decay trend is absent. Such a kind of dip-and-rise anisotropy profile indicates the presence of at least two populations of which one is the short fluorescence lifetime with fast rotational

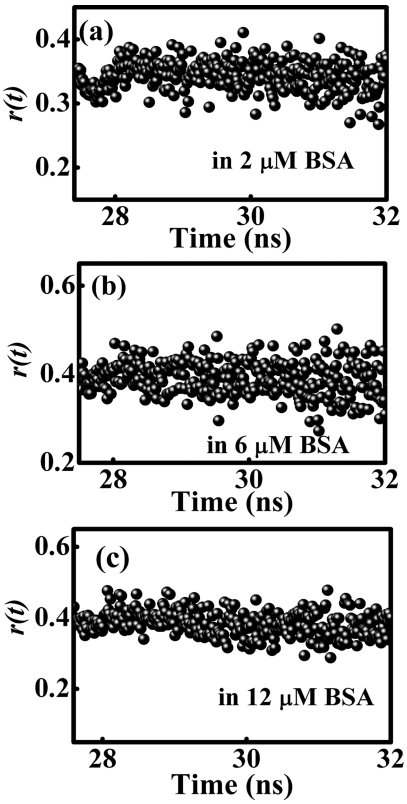

Figure 9. Time-resolved anisotropy decay profile of ADII at various BSA concentrations collected at 510 nm.

correlation time and another is the comparatively slower component in both of the cases (fluorescence lifetime and rotational correlation time).[26,40−42] Usually, this kind of anisotropy decay profile has been observed for fluorophores in confined environments like protein, DNA, etc., and the component with a shorter correlation time is attributed to the free fluorophore (i.e., fluorophore in solvent), whereas the slower component is due to the fluorophores bound to the macromolecules.[26,40−42] This kind of time-resolved anisotropy behavior can be explained with the help of a two-component anisotropy equation (eq 1), suggested by Ludescher et al.,[43] and the detailed discussion is avoided here as there are excellent reports available in the literature regarding this topic.[26,40−42] Therefore, our observed dip-and-rise kind of anisotropic decay pattern in the ADII−BSA system definitely suggests the presence of both the free and bound probe at the lower protein concentration and the disappearance of this unusual decay pattern at higher protein concentration indicates the increasing degree of the confinement of the probe. At higher protein concentration (12 μM), the obtained anisotropy decay of ADII is found to be best fitted by the single exponential function with a rotational correlation time of 8.31 ns. This high correlation time indicates the tight binding of the probe within the hydrophobic cavity of the protein BSA.[26,40]

The same time-resolved anisotropy decay of ADII has been performed in various BSA concentrations when ADII is bound to various micellar units (vide Figure S4, Supporting Information). In all cases, we obtain a monoexponential function with a rotational correlation time quite higher than that obtained in pure micellar medium and the initial anisotropy is also increased in the presence of BSA (Table S1, Supporting Information). These results strongly support

dx.doi.org/10.1021/jp504037y | J. Phys. Chem. B XXXX, XXX, XXX−XXX

our previous findings that the probe released from the corresponding micelles bind to the BSA protein. It is also found that the obtained correlation time is progressively increased with increasing BSA concentration, which suggests the strong confinement of the probe within the protein cavity. The presence of residual anisotropy in all the protein–probe systems signifies the global tumbling motion of the protein in aqueous buffer medium.[40]

3.7. Circular Dichroism (CD) and Dynamic Light Scattering (DLS) Study of BSA–ADII Complexes in Different Media. The influence of binding of the probe (ADII) on the secondary structure of the protein in aqueous buffer and in different surfactant media has been ascertained through far-UV circular dichroism (CD) studies. Figure 10

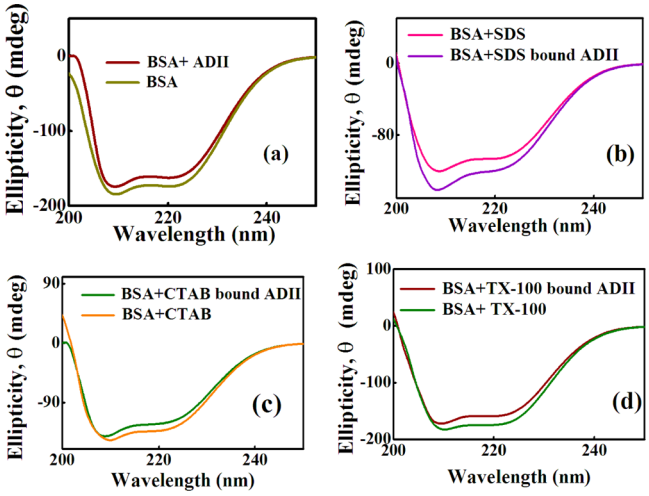

Figure 10. Far-UV circular dichroic spectral profiles of the protein ([BSA] = 20.0 μM) in the presence (a) 4 μM ADII, (b) 4 μM ADII + 7 mM SDS, (c) 4 μM ADII + 1.5 mM CTAB, and (d) 4 μM ADII + 0.35 mM TX-100 at T = 300 K in Tris–HCl buffer (pH 7.40).

shows the CD spectra of BSA–ADII composite systems in different media (aqueous buffer, SDS, CTAB, and TX-100), and the estimated α-helicity contents of BSA after binding of the probe in different media are tabulated in Table 2. A close perusal of the CD spectral results suggest that upon binding of the probe with BSA a decrement of α-helicity content of native BSA results from 67% (±2%) to 65% (±2%) in aqueous buffer medium. On the other hand, slight loss of α-helicity content is observed in TX-100 and CTAB medium, but the calculated α-helicity content of BSA in SDS medium is found to be substantially increased after probe binding which may suggest that upon binding of ADII with BSA in SDS medium a stabilizing effect in the secondary structure is produced.

Figure 11 displays the DLS spectra of BSA–ADII composite systems in different media (aqueous buffer, SDS, CTAB, and TX-100), and the obtained hydrodynamic radii (R_h) are tabulated in Table 2. The estimated hydrodynamic radius of BSA is found to be slightly increased from 3.7 to 4.1 nm in the presence of 4 μM ADII, which is also supported by the CD experiment data, as a very little unfolding of BSA native structure is found upon ADII binding in aqueous buffer medium. The hydrodynamic radii of ADI–BSA composite systems in the CTAB and TX-100 surfactant media are slightly higher than that of BSA in the respective surfactant medium, but in SDS medium, the R_h value of the ADII–BSA system is found to be smaller than that of BSA in the SDS medium.

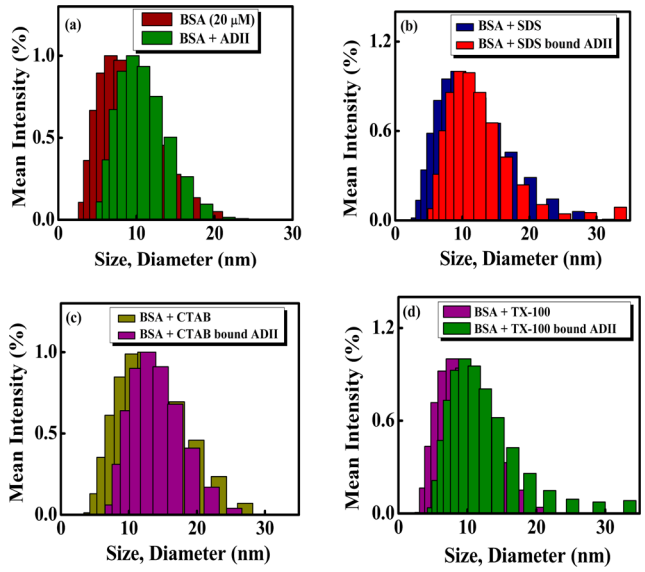

Figure 11. DLS size distribution graph for 20 μM BSA containing 4 μM ADII in (a) aqueous buffer, (b) 7 mM SDS, (c) 1.5 mM CTAB, and (d) 0.35 mM TX-100 medium.

These results coupled with the data obtained in the CD experiment suggest that in SDS medium probably refolding of BSA structure results in an increase of α-helicity content of BSA, and hence the lower hydrodynamic radius. Interestingly, the R_h value of ADII–BSA in CTAB medium is found to be in close resemblance of the hydrodynamic radius of dimeric BSA, which also justified our previous findings regarding the fact that in CTAB medium the probe binds to the dimeric BSA to form a 1:2 (ADII–BSA) stoichiometric complex (vide section 3.5).

3.8. Modeling of Probe Binding Site in BSA: Blind Docking Study. It is also a very important and crucial task to know the probable binding location of small molecular probes within the micro-heterogeneous assembly of the protein during the drug–protein binding interaction process. Here, in addition to the experimental result, the AutoDock-based blind docking technique has been employed to assess the probable binding location of the probe ADII in BSA. The AutoDock-based blind docking technique includes a search over the entire surface of the protein for binding sites and simultaneously optimizes the conformations of the peptides.[44,45] The detailed discussion of the simulation protocol has been described in section 2.3.

In the previous Experimental Section, we could not find any information regarding the binding process of the lactim form of ADII with the model transport protein BSA. As both conformers of ADII, i.e., lactim and lactam, can bind with the protein, an attempt has been undertaken to find out the binding locations of both of the isomers to the transport protein BSA and their other binding parameters theoretically. The stereo views of the minimum energy docked conformation of the lactam–BSA and lactim–BSA complexes have been displayed in Figure 12 and Figure S5 (Supporting Information). The lowest binding energy conformer has been searched out of 10 different conformations for each docking simulation. As seen from both figures, the two conformers bind to the exact same position of BSA. The protein residues in the immediate vicinity (within 4.0 Å) at the probe (lactim and lactam forms of ADII) binding locus are ARG 144, LEU 189, PRO 110, HIS 145, SER 109, SER 192, ASP 108, PRO 146, TYR 147, ALA 193, ARG 196, SER 428, ARG 458,, ILE 455, LEU 454, and ASN 457.

dx.doi.org/10.1021/jp504037y | J. Phys. Chem. B XXXX, XXX, XXX–XXX

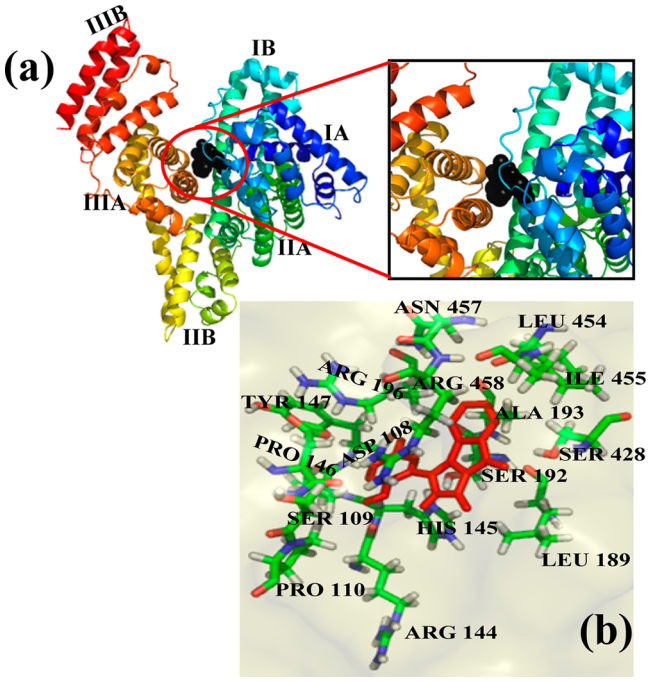

Figure 12. (a) Stereo view of the docked conformation of the lactam form of ADII with the protein BSA. A magnified view at the site of interaction of the lactam form is also shown. The drug is shown in black sphere. Panel b displays the protein residues in the near vicinity (within 4 Å) of the drug over a molecular surface representation of the protein. Color scheme: blue for nitrogen atoms, red for oxygen atoms and carbon atoms are green for protein residues and red for lactam form, and the hydrogen atoms are omitted for reasons of clarity. The pictures have been prepared with the PyMOL software package.[28]

Studying the protein residues at the immediate vicinity of the probe reveals the hydrophilic subdomain IA of the protein to be the favorable binding site for both conformers of ADII. The principal hydrophobic binding sites in BSA are located in domains II and III, while domain I is characterized by a net negative charge. Binding of the lactim and lactam forms of ADII in subdomain IA are found to be characterized by a favorable binding energy of −5.87 and −4.96 kcal/mol along with a reasonably low magnitude of the inhibition constants 49.65 and 230.63 μM, respectively. It is also found out that the hydrogen atom of the lactim form is involved in hydrogen bonding interaction with the oxygen atom of the SER 192 residue (vide Figure S5, Supporting Information).

CONCLUSION

In this article, an attempt has been made to understand the binding interaction of a potential drug template ADII with bovine serum albumin when it is released from the various micellar environments in order to understand the suitable drug delivery system. DLS study reveals that the structures of the surfactants are completely destroyed in the presence of the protein; therefore, the loaded drugs are released to the medium and ready to interact with the transport protein BSA. From the absorption study, it is clear that the CTAB-micelle-loaded anionic ADII molecule becomes neutral when it is released in BSA medium. During steady state fluorescence study, it is found that, upon encapsulation within the protein cavity, the lactam emission of ADII drastically enhances with a hypsochromic shift of emission maxima due to the conjugate effect of lower polarity and increased rigidity at the binding site of ADII imposed by the micro-heterogeneous protein environment than the bulk aqueous phase. The calculated binding constant of the probe−protein complex is enormously modified in the presence of the surfactant. It is observed that the binding of the probe in SDS medium leads to a reduction of the binding constant compared to that in the absence of the surfactant. However, in the case of CTAB medium, the binding affinity largely increases due to the formation of 1:2 (drug−protein) complex and in TX-100 medium binding constant is found to be at the same order as was found in aqueous buffer medium. Another interesting result is observed during CD experiment. It is found that upon binding of the probe within the hydrophobic cavity of BSA in SDS medium refolding of BSA secondary structure results, which is also supported by the smaller hydrodynamic radius (R_h) of the ADII−BSA system. The time-resolved fluorescence anisotropy study also supports the fact that the released probe from the different micellar units gets tightly bound with the BSA protein. Finally, the AutoDock-based blind docking simulation study recognizes that the hydrophobic subdomain IA of the protein is the probable binding site for the present drug template ADII.

ASSOCIATED CONTENT

Supporting Information

Figures showing a size distribution graph for BSA, representative time-resolved fluorescence decay profiles of ADII, representative time-resolved fluorescence decay profiles of different micelle (SDS, CTAB, and TX-100)-bound ADII, typical time-resolved fluorescence anisotropy decay profile of different micelle (SDS, CTAB, and TX-100)-bound ADII, and stereo view of the docked conformation of the lactim form of ADII with the protein BSA and the protein residues in the near vicinity of the drug over a molecular surface representation of the protein. Table showing rotational dynamical parameters of different micelle (SDS, CTAB, and TX-100)-bound ADII. This material is available free of charge via the Internet at http://pubs.acs.org.

AUTHOR INFORMATION

Corresponding Author

*Phone: +91-33-2350-8386. Fax: +91-33-2351-9755. E-mail: nguchhait@yahoo.com.

Notes

The authors declare no competing financial interest.

ACKNOWLEDGMENTS

D.R. acknowledges University Grant Commission, India, for a senior research fellowship. N.G. would like to acknowledge UPE and CRNN of CU for financial support.

REFERENCES

(1) Bodor, N. S. *Chemical Aspects of Drug Delivery Systems*; Karsa, D. R., Stephenson, R. A., Eds.; Royal Society of Chemistry: London, 1996.

(2) Gokturk, S.; Calıskan, E.; YesimTalman, R.; Var, U. A Study on Solubilization of Poorly Soluble Drugs by Cyclodextrins and Micelles: Complexation and Binding Characteristics of Sulfamethoxazole and Trimethoprim. *Sci. World J.* **2012**, *2012*, 718791.

(3) Lee, E. S.; Na, K.; Han Bae, Y. Super pH-Sensitive Multifunctional Polymeric Micelle. *Nano Lett.* **2005**, *5*, 325−329.

(4) Jin, Q.; Mitschang, F.; Agarwal, S. Biocompatible Drug Delivery System for Photo-Triggered Controlled Release of 5-Fluorouracil. *Biomacromolecules* **2011**, *12*, 3684−3691.

(5) Schmaljohann, D. Thermo- and pH-responsive polymers in drug delivery. *Adv. Drug Delivery Rev.* **2006**, *58*, 1655−1670.
(6) Zhong, D. P.; Pal, S. K.; Wang, C.; Zewail, A. H. Femtosecond dynamics of a drug−protein complex: Daunomycin with Apo riboflavin-binding protein. *Proc. Natl. Acad. Sci. U.S.A.* **2001**, *98*, 11873−11878.
(7) El-Kemary, M.; Gil, M.; Douhal, A. Relaxation dynamics of piroxicamstructures within human serum albumin protein. *J. Med. Chem.* **2007**, *50*, 2896−2902.
(8) Sakai, T.; Yamasaki, K.; Sako, K. T.; Kragh-Hansen, U.; Suenaga, A.; Otagiri, M. R. Interaction Mechanism Between Indoxyl Sulfate, a Typical Uremic Toxin Bound to Site II, and Ligands Bound to Site I of Human Serum Albumin. *Pharm. Res.* **2001**, *18*, 520−524.
(9) Peters, T., Jr. *Biochemistry Genetics and Medical Applications*; Academic Press: San Diego, CA, 1996; pp 76−132.
(10) Hodgson, J. ADMET—turning chemicals into drugs. *Nat. Biotechnol.* **2001**, *19*, 722−726.
(11) Peters, T. *All About Albumin: Biochemistry, Genetics and Medical Applications*; Academic Press: San Diego, CA, 1995.
(12) He, X.; Carter, D. C. Atomic structure and chemistry of human serum albumin. *Nature (London)* **1992**, *358*, 209−215.
(13) Carter, D. C.; Ho, J. X. Structure of serum albumin. *Adv. Protein Chem.* **1994**, *45*, 153−203.
(14) Curry, S.; Mandelkow, H.; Brick, P.; Franks, N. Crystal structure of human serum albumin complexed with fatty acid reveals an asymmetric distribution of binding sites. *Nat. Struct. Biol.* **1998**, *5*, 827−835.
(15) Valstar, A.; Almgren, M.; Brown, W. The Interaction of Bovine Serum Albumin with Surfactants Studied by Light Scattering. *Langmuir* **2000**, *16*, 922−927.
(16) Chodankar, S.; Aswal, V. K.; Kohlbrecher, J.; Vavrin, R.; Wagh, A. G. Surfactant-induced protein unfolding as studied by small-angle neutron scattering and dynamic light scattering. *J. Phys.: Condens. Matter* **2007**, *19*, 326102.
(17) Singh, S. K.; Kishore, N. Thermodynamic insight into the binding of Triton-X 100 to globular protein: a calorimetric and spectroscopic investigation. *J. Phys. Chem. B* **2006**, *110*, 9728−9737.
(18) Sharma, A.; Agarwal, P. K.; Deep, S. Characterization of different conformations of bovine serum albuminand their propensity to aggregate in the presence of N-cetyl-N,N,N-trimethylammonium bromide. *J. Colloid Interface Sci.* **2010**, *343*, 454−462.
(19) Ray, D.; Pramanik, A.; Guchhait, N. Lactim−lactam tautomerism through four member hydrogen bonded network in isoindole fused imidazole system: A combined spectroscopic and theoretical approach to photophysical properties. *J. Photochem. Photobiol., A* **2014**, *274*, 33−42.
(20) Das, S.; Fro1hlich, R.; Pramanik, A. Synthesis and Fluorescent Properties of a New Class of Heterocycles of Isoindole Fused Imidazoles with Phenolic Subunits. *Org. Lett.* **2006**, *8*, 4263−4266.
(21) Pozharskii, A. F.; Soldatenkov, A. T.; Katritzky, A. R. *Heterocycles in Life and Society*; John Wiley and Sons Ltd.: New York, 1997.
(22) Barnard, E. A.; Stein, W. D. The roles of imidazole in biological systems. *Adv. Enzymol. Relat. Subj. Biochem.* **1958**, *20*, 51−110.
(23) Boiani, M.; Gonzalez, M. Imidazole and benzimidazole derivatives as chemotherapeutic agents. *Mini-Rev. Med. Chem.* **2005**, *5*, 409−424.
(24) Jin, Z. Muscarine, imidazole, oxazole and thiazole alkaloids. *Nat. Prod. Rep.* **2005**, *22*, 196−229.
(25) Ray, D.; Pramanik, A.; Guchhait, N. Differential modulation of lactim−lactam tautomerism process of an isoindole fused imidazole system in three different assemblies of varying surface charge: a spectroscopic approach to various photophysical properties. *RSC Adv.* **2014**, *4*, 13256−13265.
(26) Lakowicz, J. R. *Principles of Fluorescence Spectroscopy*; Plenum: New York, 1999.
(27) Greenfield, N.; Fasman, G. D. Computed circular dichroism spectra for the evaluation of protein conformation. *Biochemistry* **1969**, *8*, 4108−4116.
(28) De Lano, W. L. *The PyMOL Molecular Graphics System*; De Lano Scientific: San Carlos, CA, 2002.
(29) Ghosh, S.; Jana, S.; Guchhait, N. Domain Specific Association of Small Fluorescent Probe *trans*-3-(4-Monomethylaminophenyl)-Acrylonitrile (MMAPA) with Bovine Serum Albumin (BSA) and Its Dissociation from Protein Binding Sites by Ag Nanoparticles: Spectroscopic and Molecular Docking Study. *J. Phys. Chem. B* **2012**, *116*, 1155−1163.
(30) Samanta, A.; Paul, B. K.; Guchhait, N. Spectroscopic probe analysis for exploring probe−protein interaction: A mapping of native, unfolding and refolding of protein bovine serum albumin by extrinsic fluorescence probe. *Biophys. Chem.* **2011**, *156*, 128−139.
(31) Ray, D.; Paul, B. K.; Guchhait, N. Effect of biological confinement on the photophysics and dynamics of aproton-transfer phototautomer: an exploration of excitation and emission wavelength-dependent photophysics of the protein-bound drug. *Phys. Chem. Chem. Phys.* **2012**, *14*, 12182−12192.
(32) Anand, U.; Mukherjee, S. Reversibility in protein folding: effect of *β*- cyclodextrin on bovine serum albumin unfolded by sodium dodecyl sulphate. *Phys. Chem. Chem. Phys.* **2013**, *15*, 9375−9383.
(33) Gelamo, E. L.; Tabak, M. Spectroscopic studies on the interaction of bovine (BSA) and human (HSA) serum albumins with ionic surfactants. *Spectrochim. Acta, Part A* **2000**, *56*, 2255−2271.
(34) Gelamo, E. L.; Silva, C. H. T. P.; Imasato, H.; Tabak, M. Interaction of bovine (BSA) and human (HSA) serum albumins with ionic surfactants: spectroscopy and modeling. *Biochim. Biophys. Acta* **2002**, *1594*, 84−99.
(35) Paul, B. K.; Ray, D.; Guchhait, N. Binding interaction and rotational- relaxation dynamics of a cancer cell photosensitizer with various assemblies. *J. Phys. Chem. B* **2012**, *116*, 9704−9717.
(36) Li, Y.; Yang, G.; Mei, Z. Spectroscopic and dynamic light scattering studies of the interaction between pterodontic acid and bovine serum albumin. *Acta Pharm. Sin. B* **2012**, *1*, 53−59.
(37) Du, X.; Chen, X.; Lu, W.; Hou, J. Spectroscopic study on binding behaviors of different structural nonionic surfactants to cyclodextrins. *J. Colloid Interface Sci.* **2004**, *274*, 645−651.
(38) Benesi, H. A.; Hildebrand, J. H. A Spectrophotometric Investigation of the Interaction of Iodine with Aromatic Hydrocarbons. *J. Am. Chem. Soc.* **1949**, *71*, 2703−2707.
(39) Cohen, B.; Alvarez, C. M.; Carmona, N. A.; Organero, J. A.; Douhal, A. Proton-Transfer Reaction Dynamics within the Human Serum Albumin Protein. *J. Phys. Chem. B* **2011**, *115*, 7637−7647.
(40) Sinha, S. S.; Mitra, R. K.; Pal, S. K. Temperature-Dependent Simultaneous Ligand Binding in Human Serum Albumin. *J. Phys. Chem. B* **2008**, *112*, 4884−4891.
(41) Paul, B. K.; Guchhait, N. Modulated Photophysics of an ESIPT Probe 1-Hydroxy-2-naphthaldehyde within Motionally Restricted Environments of Liposome Membranes Having Varying Surface Charges. *J. Phys. Chem. B* **2010**, *114*, 12528−12540.
(42) Bhattacharya, B.; Nakka, S.; Guruprasad, L.; Samanta, A. Interaction of Bovine Serum Albumin with Dipolar Molecules: Fluorescence and Molecular Docking Studies. *J. Phys. Chem. B* **2009**, *113*, 2143−2150.
(43) Ludescher, R. D.; Peting, L.; Hudson, S.; Hudson, B. Time-resolved fluorescence anisotropy for systems with lifetime and dynamic heterogeneity. *Biophys. Chem.* **1987**, *28*, 59−75 and references therein.
(44) Hetenyi, C.; van der Spoel, D. Blind docking of drug-sized compounds to proteins with up to a thousand residues. *FEBS Lett.* **2006**, *580*, 1447−1450.
(45) Campbell, S. J.; Gold, N. D.; Jackson, R. M.; Westhead, D. R. Ligand binding: functional site location, similarity and docking. *Curr. Opin. Struct. Biol.* **2003**, *13*, 389−395.